FEBS Letters 581 (2007) 637–643

Metabolism of glutathione in tumour cells as evidenced by 1H MRS

S. Grande[a], A.M. Luciani[a], A. Rosi[a], A. Palma[a], C. Giovannini[b], O. Sapora[c], L. Guidoni[a], V. Viti[a,*]

[a] Dipartimento Tecnologie e Salute and INFN Gruppo Collegato Sanita', Istituto Superiore di Sanita', Viale Regina Elena 299, 00161 Roma, Italy
[b] Centro Nazionale per la Qualità degli Alimenti e per i Rischi Alimentari, Istituto Superiore di Sanita', Viale Regina Elena 299, 00161 Roma, Italy
[c] Dipartimento di Ambiente e Connessa Prevenzione Primaria, Istituto Superiore di Sanita', Viale Regina Elena 299, 00161 Roma, Italy

Received 12 December 2006; revised 11 January 2007; accepted 12 January 2007

Available online 18 January 2007

Edited by Miguel De la Rosa

Abstract **1H MRS signals of glutathione and of free glutamate were examined in samples from cultured tumour cells, namely MCF-7 from mammary carcinoma and TG98 from malignant glioma, with the aim of relating signal intensities to aspects of GSH metabolism. Spectra of cells harvested at different cell densities suggest that GSH and glu signal intensities are related to cell density and proliferation and their ratio is dependent on the activity of the γ-glutamyl cysteine synthetase. The hypothesis is confirmed by experiments performed on cells treated with buthionine sulfoximine that inhibits the enzyme activity.**
© 2007 Federation of European Biochemical Societies. Published by Elsevier B.V. All rights reserved.

Keywords: 1H MRS; Glutathione; γ-Glutamyl cysteine synthetase; Tumour cells

1. Introduction

The tripeptide γ-glutamylcysteinylglycine, Glutathione (GSH), is a ubiquitous molecule that may act as antitoxic agent by reacting with both electrophylic or oxidizing species [1]. The GSH level and metabolism have been invoked as major determinants of the efficiency of cells in its detoxification action against internal toxic agents that are produced during cell lifespan as well as external chemical or physical insults [2].

MRS has been employed to study GSH metabolism both in vitro [3,4] and in vivo [5,6]. 1H MRS signals of GSH and of its oxidized form GSSG were assigned to specific chemical groups through 1D and 2D COSY experiments performed in GSH solution and in perchloric acid extracts from tissues [4,7,8].

In a previous paper [8], we related the intensity of GSH signals of tumour cells to cell tendency to undergo apoptosis by irradiation. In the present study, we examined MRS signal intensity of GSH and of free glu in cultured cells MCF-7 from mammary carcinoma and T98G from malignant glioma, aiming at elucidating to which aspects of GSH metabolism they are related. On the basis of experiments on cells collected at different cell densities and on cells treated with buthionine sulfoximine (BSO), we found that the cell density and proliferation are the major determinant of intensities of GSH and of free glu signals and their ratio is directly related to the activity of γ-glutamyl cysteine synthetase, the rate limiting enzyme in GSH synthesis.

2. Materials and methods

MCF-7 cells were purchased from ATCC (Manassas, VA, USA) and kindly donated by Dr. Stefania Meschini, Istituto Superiore di Sanità, Rome, Italy. Cells were grown, as adherent cells, in RPMI 1640 medium (Hyclone, Logan, Utah) and 1× nonessential aminoacids (Euro Clone Life Science Division, Milan, Italy). T98G cells were purchased from the ECACC (Porton Down, Salisbury, Wiltshire, SP4 0JG) and kindly donated by Dr. Angelica Facoetti of University of Pavia, Italy. Cells were grown, as adherent cells, in RPMI 1640 medium (Hyclone) added with 1 mM sodium pyruvate and 1× nonessential amino acids (Euro Clone Life Science Division). The medium of both cell lines was supplemented with 10% fetal calf serum (Hyclone) and 50 μg/ml gentamicin. Cells deriving from both cell lines were routinely seeded in 175 cm^2 flasks at a density of 4×10^5 cells per flask in 50 ml medium. The medium was replaced every 72 h.

MCF-7 and T98G cells were treated with BSO for 18 h. The medium was then removed, cells washed and fresh medium added.

GSH solutions were prepared by dissolving GSH in ^2H_2O to a final concentration of 10 mM and pH adjusted to 7.4.

PCA extracts were prepared as previously described [8].

All reagents were purchased from Sigma (St. Louis, MI, USA).

1D 1H MR spectra were run at 400.14 MHz on a digital Avance spectrometer (Bruker, AG, Darmstadt, Germany) equipped with a 1 mm microprobe. Signals were acquired with a 90° RF pulse and a sweep width of 4006.4 Hz. The number of scans was 512 with a repetition time of 4.36 s. Water suppression was obtained by irradiating water signal. 2D 1H COSY spectra of cells were acquired with a 90°–tl–90°–t2 pulse sequence, by summing 16 free induction decays for each of 256 increments in t1. Spectra were acquired as a matrix of 512×256 data points in the time domain. When indicated, a Lorentzian–Gaussian function with LB = −10 Hz and GB = 0.1 was applied to enhance the resolution in the time domain before Fourier transformation.

To perform MRS measurements on cells, a pellet of approximately 5×10^6 cells was suspended in phosphate-buffered saline with 10% ^2H_2O and inserted in a 1 mm tube.

By considering that (i) the spectral region of interest was well characterized with respect to metabolite peaks; (ii) signals had similar intensities and linewidths and (iii) the signal to noise ratio was above 10 also for the lowest signals, the "1D WINNMR" software (Bruker) was considered adequate for spectral deconvolution. A Gaussian/Lorentzian ratio equal to 1 for the line shape function was chosen.

3. Results

Fig. 1 shows the 1H MR spectral regions (4.5–0.5 ppm) of T98G (a) and of MCF-7 (b) cells. Many signals from mobile lipids are present in both spectra. Main signals of fatty acid

*Corresponding author. Fax: +39 06 49387075.
E-mail address: viti@iss.it (V. Viti).

0014-5793/$32.00 © 2007 Federation of European Biochemical Societies. Published by Elsevier B.V. All rights reserved.
doi:10.1016/j.febslet.2007.01.025

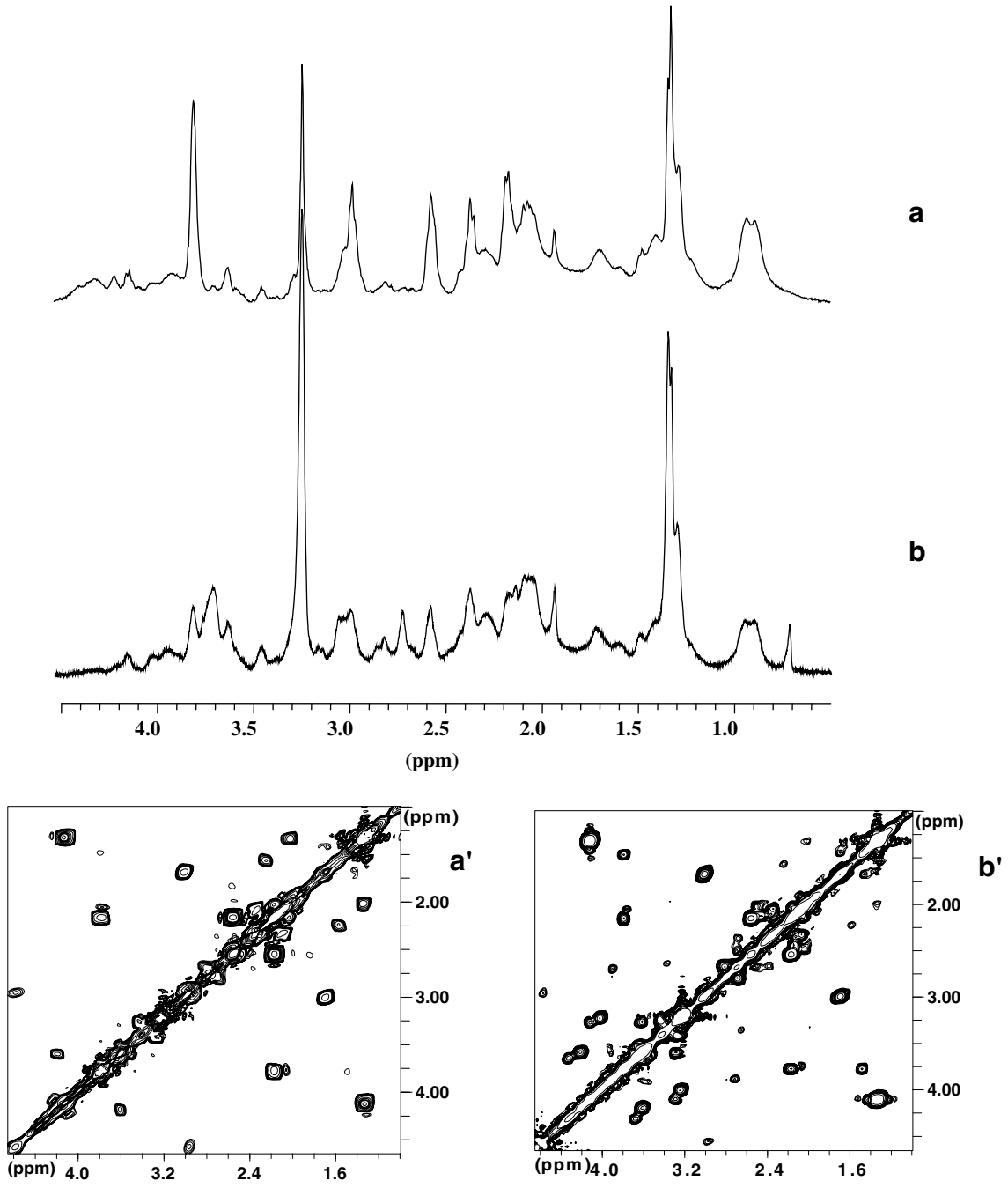

Fig. 1. ID 1H MR spectra (region 4.5–0.5 ppm) of (a) T98G and (b) MCF-7cells. 2D COSY 1H MR spectra (region 4.65–1 ppm) of (a′) T98G and (b) MCF-7 cells.

chains are at 0.89 ppm from terminal $–CH_3$, at 1.27 ppm from $(–CH_2)_n$ bulk, at 1.61 ppm from $(–CH_2)$ in position 3, at 2.02 ppm from CH_2—C**H**$_2$—CH=CH and at 2.32 ppm from $(–CH_2)$ in position 2. Signals from GSH, centred at 2.97 (βCH_2 group of cys), 2.55 (γCH_2 of glu), 2.17 (βCH_2 of glu) are also intense, particularly in spectra of T98G cells (Fig. 1a). Signals at 2.35 and at 2.10 ppm are from γCH_2 and βCH_2 of free glu, respectively. Assignments were confirmed by 2D COSY spectra (Fig. 1a′,b′). The correlations from glu residues in GSH can be found at 2.17–2.55 ppm (β and γ protons) and at 2.17–3.78 ppm (β and α protons). The cross peak of cys residue in GSH is found at 2.97–4.57 ppm (β and α protons). Free glu shows the cross peak at 2.10–2.35 ppm from β and γ protons, while the correlation from β and α protons at 2.10–3.77 ppm partially overlaps to the corresponding cross peak of glu in GSH.

To perform signal deconvolutions for evaluating intensities of signals associated to the GSH metabolism, we compared cell spectra with those of GSH and of free glu solutions. Fig. 2 shows the 1H MR spectral regions, diagnostic for GSH and free glu signals, of a T98G cell sample (a), GSH solution (b) and glu solution (c). The structure of the signals at 2.55 at

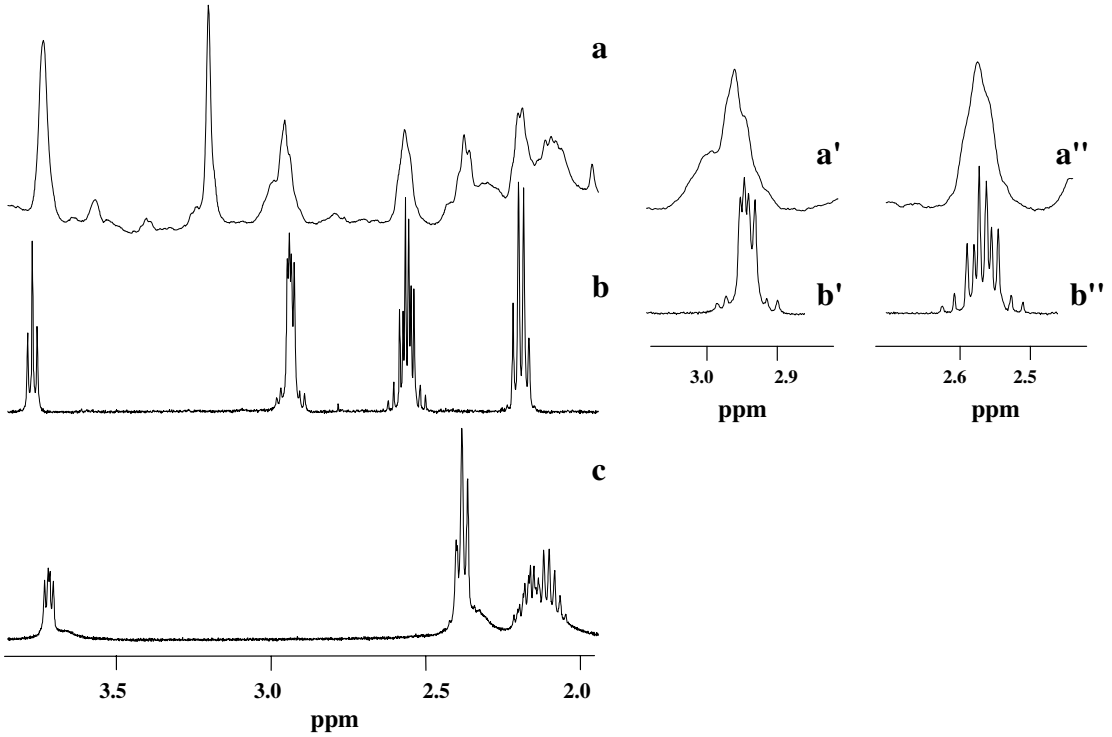

Fig. 2. (a) Spectrum (region 3.9–1.9 ppm) of T98G cells with (a′,a″), details of cys and glu of GSH, respectively; (b) spectrum (region 3.9–1.9 ppm) of 10 mM GSH solution with (b′,b″). details of cys and glu of GSH, respectively; (c) spectrum (region 3.9–1.9 ppm) of 10 mM glu solution.

2.97 ppm is shown in more detail in Fig. 2a′,a″,b′,b″. Comparison of GSH signals in cells with GSH signals in solution indicates that the envelope of glu in GSH, resulting from the coupling pattern of the two protons of γCH_2 with the two protons of βCH_2, resonates approximately at the same frequency in cell and in solution spectra (compare Fig. 2a″,b″). On the contrary, the cys envelope, resulting from the coupling pattern of the two protons of βCH_2 with the proton of αCH group, is shifted in cell spectra to higher fields with respect to the same signal in GSH solution (compare Fig. 2a′,b′).

Peak deconvolution of cell spectra that takes into account coupling patterns deriving from spectra of GSH and glu solutions, is shown in Fig. 3. The cys peak of GSH was fitted with five lines and three further lines at lower fields (at 3.04, at 3.03 and 3.01 ppm, respectively) were added in both T98G (Fig. 3a) and MCF7 cell spectra (not shown). On the basis of a comparison with PCA extract spectra (not shown), the signal at 3.04 ppm was attributed to the CH_2 of creatine (more intense in MCF7 than in T98G cells and extracts) and the signal at 3.01 ppm to the εCH_2 of Lys (of comparable intensity in the two cell lines). The signal at 3.03 ppm was not assigned. The signal of glu of GSH at 2.55 ppm was fitted with eight lines (Fig. 3b). Fourteen lines were necessary to obtain a good fit in the interval 1.5–2.5 ppm (Fig. 3c). In particular, quartets were used to fit the free glu peak at 2.35 ppm and the peak of glu of GSH at 2.17 ppm while one large peak was used to fit the envelope centred around 2.10 ppm deriving from the βCH_2 of free glu and gln (the γCH_2 of gln is the peak at 2.42 ppm). The peak at 1.9 is from the acetate while the peak at 1.68 was not assigned. Fig. 3d shows the 0.4–1.20 ppm region deconvolved with one peak at 0.94 ppm from cytosolic polypeptides, at 0.89 ppm from cytosolic polypeptides and lipids and at 0.7 ppm from cholesterol. Finally, a broad component encompassing the deconvolved regions was added.

To measure relative metabolite concentrations, fitted peak areas in the 1D spectra were referred to the area of the signal at 0.94 ppm from the methyl group of cytosolic polypeptides. We indicate with G the relative concentration of GSH in cells measured by the envelope signal intensity of glu of GSH at 2.55 ppm and with g that of free glu at 2.35 ppm while "glutot" indicates the sum $G + g$. Furthermore, we indicate with C the relative concentration of cys of GSH measured from the envelope signal intensity at 2.97 ppm. Table 1 reports relative concentrations G, C, g and glutot and ratios G/g and C/G for a number of samples deriving from cells harvested in log phase. Notably, C was only 76% of G in MCF-7 cells and 85% of G in T98G cells, pointing to an incomplete visibility of cys of GSH in cell spectra.

Cell growth slowed down as cell density increased during progression towards confluent and post confluent state for both MCF-7 and T98G cells (Fig. 4a,b). G decreased as a function of the time in culture in both cell lines (Fig. 4a′,b′) and its decrease was accompanied by a parallel decrease of g and glutot while ratios G/g were almost constant up to six days after seeding (Fig. 4a′,a″,b′,b″). Afterwards, in correspondence with the onset of confluence, g remained almost constant while G further decreased: consequently, G/g ratios dropped to lower values (Fig. 4a′,a″,b′,b″).

A large spread of G and g values was observed in different samples harvested from MCF-7 and T98G cells in log phase. Nevertheless, both G and g were linearly dependent on glutot (Fig. 5a,b) while ratios G/g were almost constant (Fig. 5a′,b′).

To clarify to which metabolic steps the signal intensity changes could be attributed, we monitored the effect of

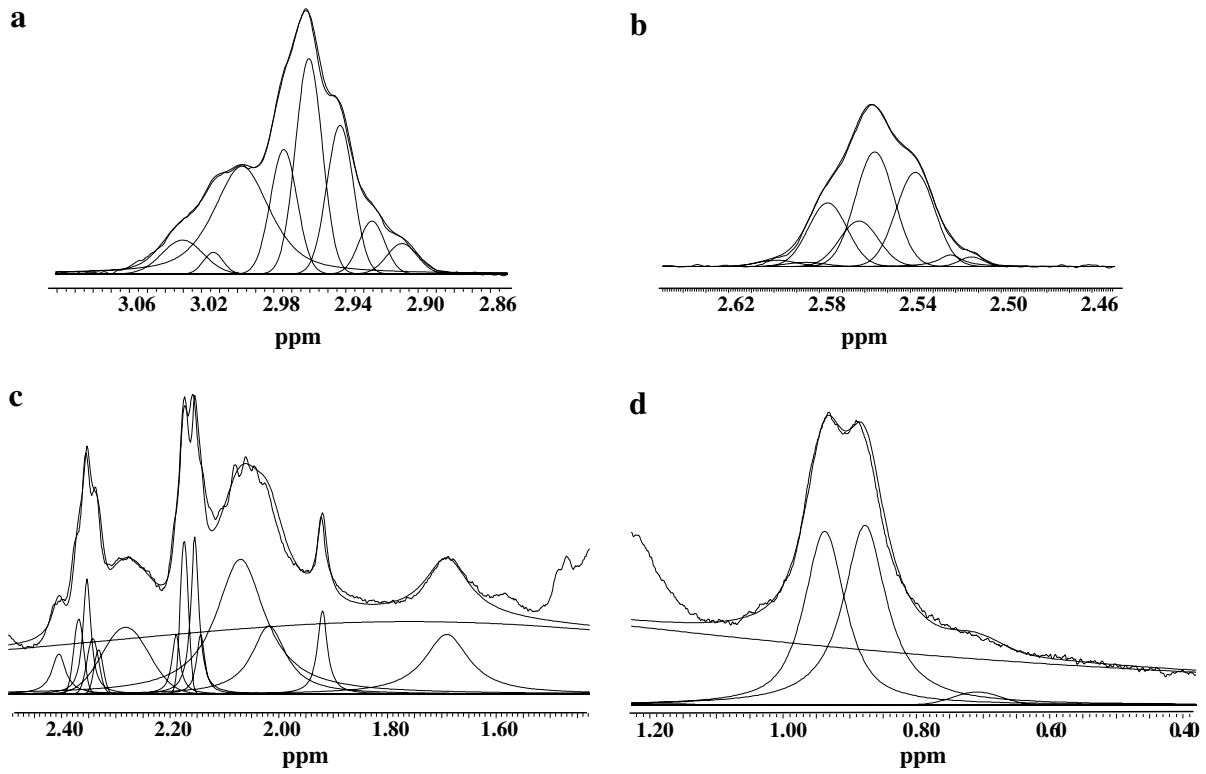

Fig. 3. Spectral deconvolution of a typical ^{1}H MR spectrum of T98G cells: (a) region of cys of GSH; (b) region of glu of GSH; (c) region of free glu; (d) region of the cytosolic polypeptides. See text for signal assignments.

Table 1
Mean values and standard deviation (in brackets) of relative concentrations of glu of GSH (*G*), free glu (*g*), glutot = *G* + *g* and cys of GSH (*C*) as obtained from spectra of MCF-7 and T98G cells (at least 10 independent experiments)

	MCF-7	T98G
G	0.74 (0.12)	0.84 (0.25)
g	0.71 (0.19)	0.54 (0.14)
Glutot	1.45 (0.12)	1.38 (0.38)
G/*g*	1.04 (0.51)	1.54 (0.19)
C	0.56 (0.02)	0.85 (0.15)
C/*G*	0.78 (0.12)	0.85 (0.15)

Ratios among values are also given. Cells had been harvested in log phase.

inhibiting the activity of γ-glutamyl cysteine synthetase on MR signals. Cell were treated with BSO, that inhibits the enzyme activity, and Fig. 6 shows a representative experiment of dose response with BSO concentration ranging from 0.025 to 1 mM. In MCF-7 cells, treatment with 0.1 mM BSO concentration produced a decrease of *G* up to 46% of control sample, paralleled by an increase of *g* (Fig. 6a and Table 2). *G* decreased further in this cell line by increasing BSO concentration to 1 mM, representing an additional drop of 10% (Fig. 6a and Table 2). T98G cells were even more sensitive to BSO as *G* decreased to 16% of control for 0.1 mM BSO concentration: a further 9% decrease was induced by 1 mM BSO. Also in T98G cells, *g* increased (Fig. 6b). As a consequence, *G*/*g* ratio markedly decreased in both cell lines (Fig. 6a′,b′). The increase of *g* did not compensate completely the decrease of *G* and, consequently, glutot values were lower in treated with respect to controls (Table 2) in both cell lines. Furthermore, BSO treated samples were characterized by a lower number cells with respect to controls (Table 2).

Analysis of 2D COSY spectra confirmed the behaviour of the 1D spectra. On the other hand, they were not considered for evaluating metabolite relative concentrations because cross peak areas are strongly dependent on relaxation times.

4. Discussion

MRS technique is presently employed to monitor GSH concentration particularly in in vivo studies [6]. A deep insight into the meaning of intensity changes of MRS signals associated to GSH metabolism is therefore of fundamental importance. With this respect, studies in intact cultured cells that maintain cells under controlled conditions are a unique tool for highlighting aspects of GSH metabolism.

The literature data report decrease of GSH level when cell density increases [9–11]. Our MRS data confirm the literature findings, as the relative concentration of GSH, *G*, decreased with time in culture in both MCF-7 and T98G cells (Fig. 4). These data were completed by the new observation that a comparable decrease occurred also for the concentration of free glu, *g*, in log phase (Fig. 4). Consequently, the concentration of total glu, glutot, decreased while ratios *G*/*g* remained almost constant in log phase. *G*/*g* was affected only at confluence (Fig. 4).

In the past, it was not clear whether the decrease of GSH with cell density increase was due to limited nutrient supply or to programmed regulation. In our opinion, the decrease

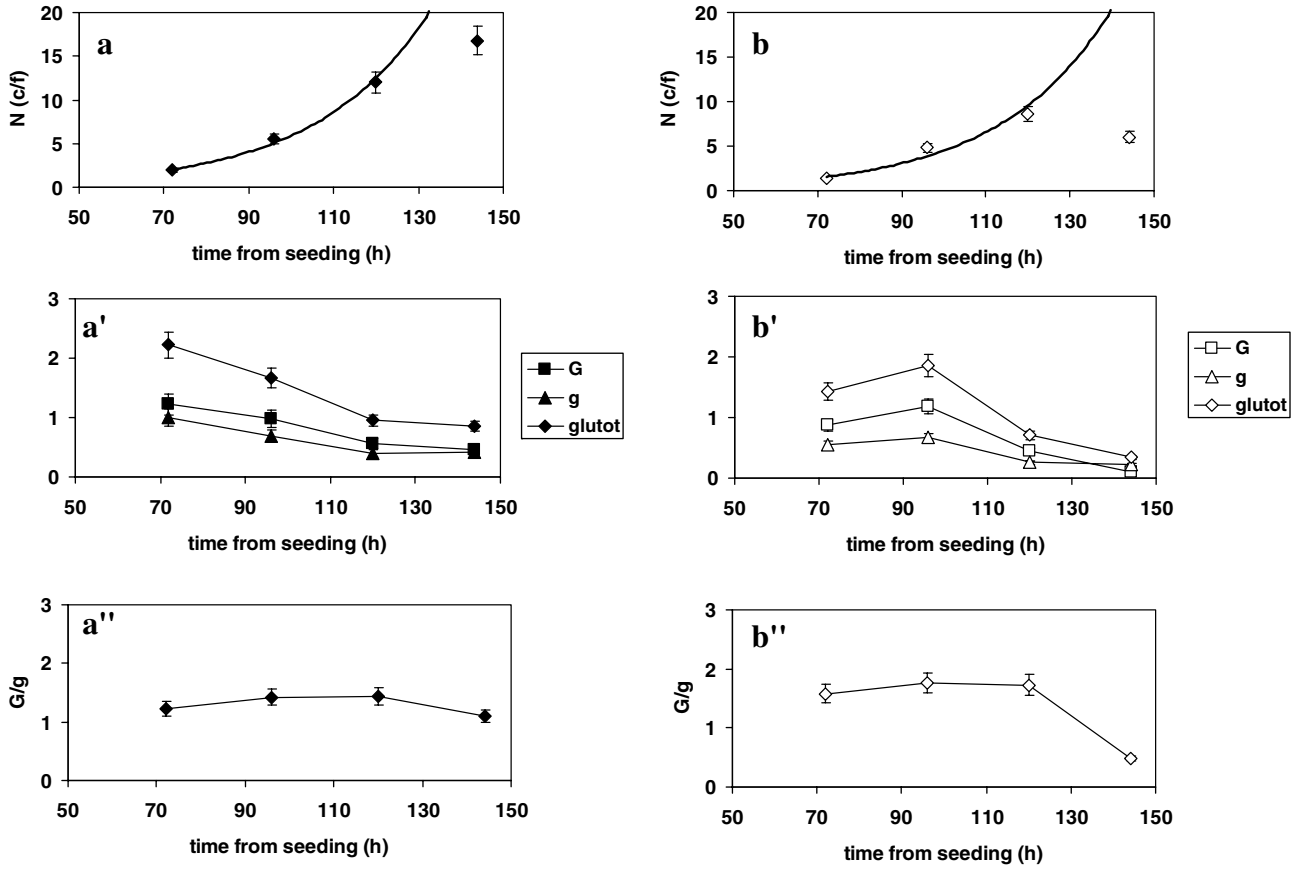

Fig. 4. Growth curves of (a) MCF-7 and (b) T98G, respectively, as a function of time (hours, h) from seeding. N indicates the number of cells ($\times 10^{-6}$) harvested from culture flasks (c/f) and lines are the exponential model for cells in log phase; relative concentrations G of glu in GSH, g of free glu, and glutot = $G + g$, as a function of time (hours, h) from seeding for (a′) MCF-7 and (b′) T98G cells; G/g ratios as a function of time (hours, h) from seeding for (c) MCF-7 and (c′) T98G cells. Lines in a′,a″,b′,b″ are merely to guide the eye. Reported values are relative to a single representative experiment for MCF-7 and one for T98G cells.

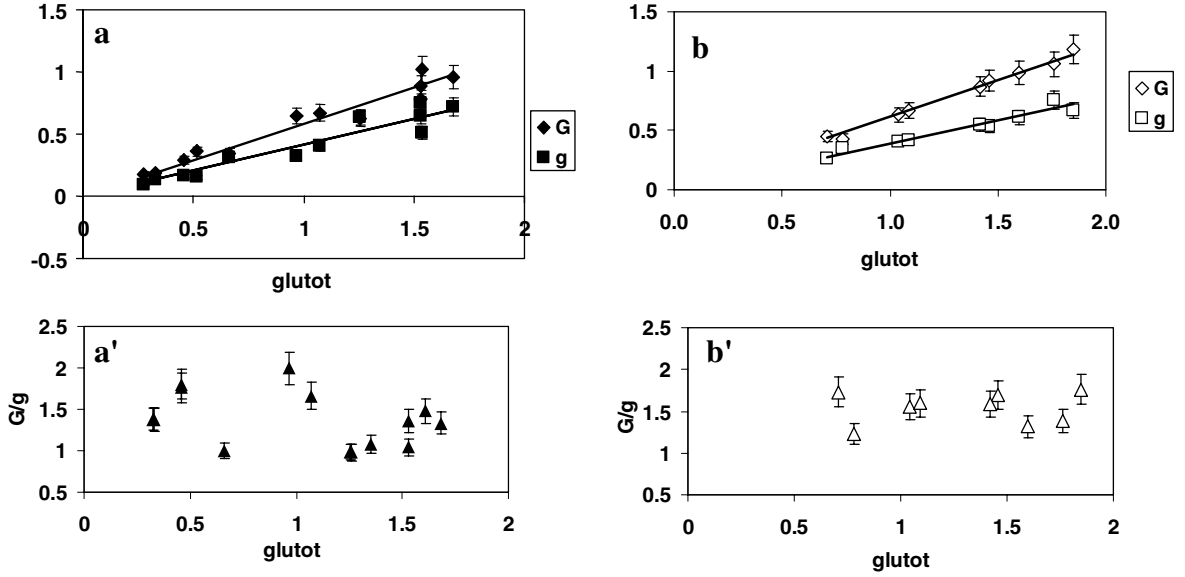

Fig. 5. Relative concentrations G, of glu of GSH and g of free glu as a function of totglu = $G + g$ concentration in a number of uncorrelated experiments performed with cells harvested in log phase for (a) MCF-7 and (b) T98G cells (lines are linear regressions); G/g ratios as a function of totglu concentration in the same experiments, for (a′) MCF-7and (b′) T98G cells.

of G accompanied by the decrease of g (and therefore of glutot) with cell density in log phase may be attributed to a decrease of the amount of nutrients that cells draw from the medium, amount that is mostly bound to cell crowding and

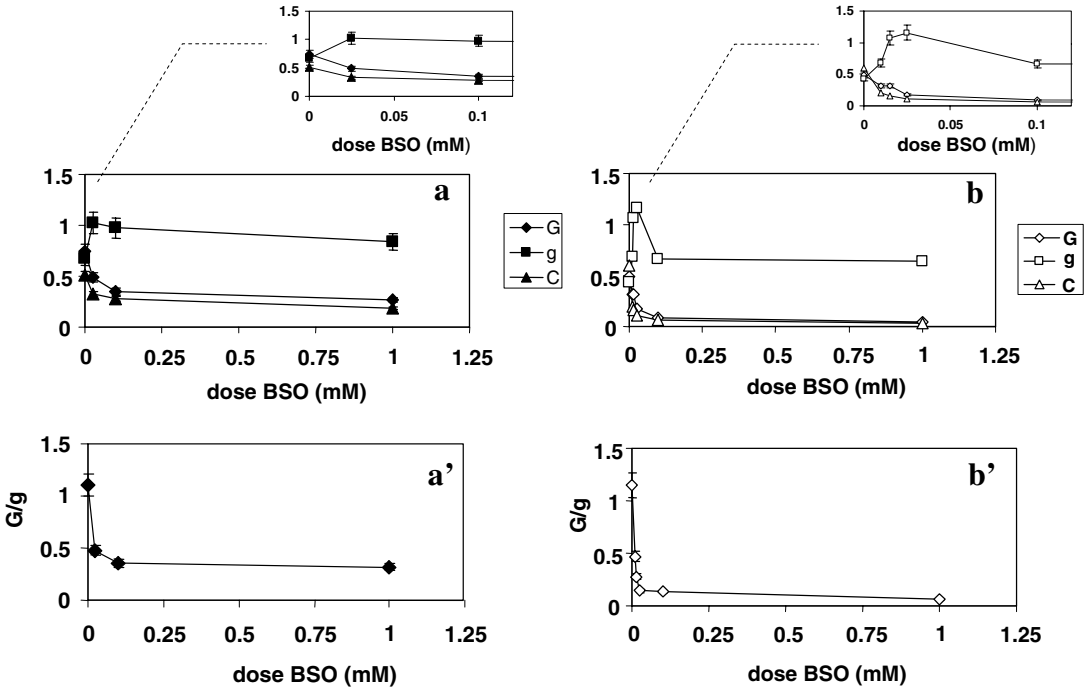

Fig. 6. Relative concentrations *G*, of glu of GSH, *C* of cys of GSH and *g* of free glu in BSO treated (a) MCF-7 and (b) T98G cells, as a function of BSO concentration. *G*/*g* ratios as a function of BSO concentration in the same experiments for (a′) MCF-7and (b′) T98G cells. Lines in a,a′,b,b′ are merely to guide the eye. Reported values are relative to a single representative experiment.

Table 2
Mean values of relative concentrations of glu of GSH (*G*), free glu (*g*) and glutot = *G* + *g* obtained from spectra of MCF-7 and T98G cells after treatment with BSO at the indicated concentrations

	MCF-7	MCF-7 0.1 mM BSO tr	MCF-7 1 mM BSO tr
N (c/f)	10.5 ± 1	7.1 ± 0.7	8 ± 0.8
G	0.74 ± 0.07	0.34 ± 0.03	0.27 ± 0.03
g	0.71 ± 0.07	0.98 ± 0.1	0.97 ± 0.1
glutot	1.45 ± 0.15	1.27 ± 0.13	0.83 ± 0.08
	T98G	T98G 0.1 mM BSO tr	T98G 1 mM BSO tr
N (c/f)	2.5 ± 0.3	2.2 ± 0.2	1.5 ± 0.2
G	0.49 ± 0.05	0.09 ± 0.009	0.040 ± 0.004
g	0.43 ± 0.04	0.66 ± 0.07	0.64 ± 0.06
glutot	0.92 ± 0.09	0.75 ± 0.08	0.68 ± 0.07

Cells, seeded at a density of 4×10^5 cells per flask, had been BSO treated at the third day in culture and harvested 18 h after treatment. The number $N \times 10^{-6}$ of cells per flask (c/f) is also given. Data reported are from one representative experiment for MCF-7 and one for T98G.

is unpredictable from one experiment to another (Fig. 5). On the other hand, constant *G*/*g* ratios during cell proliferation in log phase should reflect the constant activity of the enzyme γ-glutamylcysteine synthetase while the decrease of *G* not accompanied by a decrease of *g* and the consequent drop of *G*/*g* observed at confluence (Fig. 4) could be due to lower activity of this enzyme when cells are less proliferating.

This interpretation is confirmed by the pattern of signal intensity modifications of MCF-7 and T98G cells after BSO treatment. After inhibiting the activity of the γ-glutamylcysteine synthetase by BSO, in fact, *G* decrease was accompanied by increase of *g* with a consequent strong decrease of *G*/*g* ratios (Fig. 6 and Table 2). This effect was dose dependent (Fig. 6 and Table 2) and is due to the lower activity of the γ-glutamylcysteine synthetase. This enzyme, being the rate limiting step in the GSH synthesis, hinders the utilization of glu that cells draw from the medium for GSH synthesis. *G*/*g* ratio can be, therefore, utilized as an index of the activity of γ-glutamylcysteine synthetase, the rate limiting enzyme in GSH synthesis that is constant in log phase and declines passing from log to confluent state.

On the other hand, glutot declined slightly as a function of BSO dose because the increase of *g* did not compensate the decrease of *G* (Table 2). By observing that the number of cells in treated samples was slightly lower than in controls (Table 2), a lower proliferation rate in BSO treated cells can be envisaged, in agreement with evidences from the literature [12]. The slight decrease of glutot in BSO-treated cells could be therefore consequence of this decreased proliferation. Cell cycle modifications linked to lower proliferation after BSO treatment have been observed in different cell systems [13]. Preliminary data (not shown) indicate a similar behaviour for the cell lines here examined.

Intensity of cys signal is approximately 76% of glu signal in GSH of MCF-7 cells and 85% in GSH of T98G cells (Table 1). The cys residue in GSH can be strongly involved in interactions with other molecules: in fact, protein *S*-glutathionylation is a well-described phenomenon occurring in a number of relevant physiologically situations [2]. The presence of very strong interactions that immobilize the cys residue in a pool of GSH molecules may account for the lack of visibility in the MR spectra. On the other hand, the chemical shift of the cys signal is different in cell spectra with respect to GSH solution (Fig. 2), showing that also the visible pool of cys is affected by some kind of interactions.

The glu residue and the visible cys residue in GSH are affected by treatment with BSO in a twofold manner in both cell lines (Fig. 6). This result suggests that there are two pools of GSH in the cell, with one easily depleted by BSO and a second more resistant. The entity of the two pools depends on the cell line. This behaviour would confirm the hypothesis of the literature that a pool of GSH exists, more resistant to BSO treatment, attributed mostly to mitochondrial GSH [14–16].

These evidences, if confirmed in other cell systems, may offer a new tool for the study of GSH metabolism.

Acknowledgement: This work has been performed in the framework of the experiment EPICA of the INFN.

References

[1] Meister, A. and Anderson, M.E. (1983) Glutathione. Ann. Rev. Biochem. 52, 711–760.
[2] Masella, R., Di Benedetto, R., Vari, R., Filasi, C. and Giovannini, C. (2005) Novel mechanisms of natural antioxidant compounds in biological systems: involvement of glutathione and glutathione-related enzymes. J. Nutrit. Biochem. 16, 577–586.
[3] Gamcsik, M.P., Dubay, G.R. and Cox, B.R. (2002) Increased rate of glutathione synthesis from cystine in drug-resistant MCF-7 cells. Biochem. Pharmacol. 63, 843–851.
[4] Moreno, A. and Arus, C. (1996) Quantitative and qualitative characterization of 1H NMR spectra of colon tumors, normal mucosa and their perchloric acid extracts: decreased levels of myo-inositol in tumors can be detected in intact biopsies. NMR Biomed. 9, 33–45.
[5] Mueller, S.G., Trabesinger, A.H., Boesiger, P. and Wieser, H.G. (2001) Brain glutathione levels in patients with epilepsy measured by in vivo (1)H-MRS. Neurology 57, 1422–1427.
[6] Opstad, K.S., Provencher, S.W., Bell, B.A., Griffiths, J.R. and Howe, F.A. (2003) Detection of elevated glutathione in meningiomas by quantitative in vivo ^{1}H MRS. Magn. Reson. Med. 49, 632–637.
[7] Koga, N., Inskeep, P.B., Harris, T.M. and Guengerich, F.P. (1986) *S*-[2(*N*-guanyl)ethyl]glutathione, the major DNA adduct formed from 1,2-dibromoethane. Biochemistry 25, 2192–2198.
[8] Rosi, A, Grande, S., Luciani, A.M., Palma, A., Giovannini, C., Guidoni, L., Sapora, O. and Viti, V. (in press) Role of glutathione in apoptosis induced by radiation as determined by 1H MR spectra of cultured tumor cells. Radiat. Res.
[9] Grande, S., Luciani, A.M., Rosi, A., Cherubini, R., Conzato, M., Guidoni, L. and Viti, V. (2001) Radiation effects on soluble metabolites in cultured HeLa cells examined by ^{1}H MRS: changes in concentration of glutathione and of lipid catabolites induced by gamma rays and protons beams. Int. J. Cancer (Radiat. Oncol. Invest) 96 (S), 27–42.
[10] Chen, J., Small-Howard, A., Yin, A. and Berry, M.J. (2005) The response of Ht22 cells to oxidative stress induced by buthionine sulfoximine (BSO). BMC Neurosci. 6, 10–17.
[11] Yanagisawa, T., Urade, M., Takahashi, Y., Yamamoto, Y. and Furuyama, J. (1997) Levels of superoxide dismutases, glutathione, and poly(ADP-ribose) polymerase in radioresistant human KB carcinoma cell line. Jpn. J. Cancer Res. 11, 1070–1077.
[12] Menon, S.G. and Goswami, P.C. (2006) A redox cycle within the cell cycle: ring in the old with the new. Oncogene, 1–9.
[13] Schnelldorfer, T., Gansauge, S., Schlosser, S., Beger, H.G. and Nussler, A.K. (2000) Glutathione depletion causes cell growth inhibition and enhanced apoptosis in pancreatic cancer cell. Cancer 89, 1440–1447.
[14] Seyfred, J., Soldner, F., Schulz, J.B., Klockgether, T., Kovar, K.A. and Wullner, U. (1999) Differential effects of BSO and ethacrynic acid on glutathione levels and mitochondrial function in PC12 cells. Neurosci. Lett. 264, 1–14.
[15] Roychowdhury, S., Wolf, G., Keilhoff, G. and Horn, T.F. (2003) Cytosolic and mitochondrial glutathione in microglial cells are differentially affected by oxidative/nitrosative stress. Nitric oxide 8, 39–47.
[16] Green, R.M., Graham, M., O'Donovan, M.R., Chipman, J.K. and Hodges, N.J. (2006) Subcellular compartmentalization of glutathione: correlations with parameters of oxidative stress related to genotoxicity. Mutagenesis 21, 383–390.